A Renewed Capability for Gas Puff Science on Sandia's Z Machine

Brent Jones, *Member, IEEE,*Christopher A. Jennings, Derek C. Lamppa, Stephanie B. Hansen, Adam J. Harvey-Thompson, David J. Ampleford, Michael E. Cuneo, *Senior Member, IEEE,*Thomas Strizic, Drew Johnson, Michael C. Jones, Nathan W. Moore, Timothy M. Flanagan, John L. McKenney, Eduardo M. Waisman, Christine A. Coverdale, *Fellow, IEEE,* Mahadevan Krishnan, Philip L. Coleman, Kristi Wilson Elliott, Robert E. Madden, John Thompson, Alex Bixler, *Member, IEEE,*J. Ward Thornhill, John L. Giuliani, *Member, IEEE,*Young K. Chong, Alexander L. Velikovich, Arati Dasgupta, and J. P. Aprusese

(Invited Paper)

***Abstract*— A comprehensive gas puff capability is being developed on the Z pulsed power generator. We describe the methodology employed for developing a gas puff load on Z, which combines characterization and modeling of the neutral gas mass flow from a supersonic nozzle, numerical modeling of the implosion of this mass profile, and experimental evaluation of these magnetic implosions on Z. We are beginning a multi-year science program to study gas puff z-pinch physics at high current, starting with an 8-cm-diameter double-shell nozzle which delivers a column of Ar gas that is imploded by the machine's fast current pulse. The initial shots have been designed using numerical simulation with two radiation-magnetohydrodynamic codes. These calculations indicate that 1 mg/cm should provide optimal coupling to the driver and 1.6:1 middle:outer shell mass ratio will best balance the need for high implosion velocity against the need to mitigate the magnetic Rayleigh-Taylor instability. The models suggest 300-500 kJ Ar K-shell yield should be achievable on Z, and we report an initial commissioning shot at lower voltage in which 250 kJ was measured. Future experiments will pursue optimization of Ar and Kr K-shell x-ray sources, study fusion in deuterium gas puffs, and investigate the physics of gas puff implosions including energy coupling, instability growth, and radiation generation.**

***Index Terms*— Plasma pinch, gas puff, supersonic nozzle, X-ray production, K-shell radiation, magnetohydrodynamics (MHD).**

Manuscript received July 5, 2013; revised XXX YYY, 2013. This work was supported by Sandia National Laboratories, a multi-program laboratory managed and operated by Sandia Corporation, a wholly owned subsidiary of Lockheed Martin Corporation, for the U.S. Department of Energys National Nuclear Security Administration under contract DE-AC04-94AL85000.

B. Jones, C. A. Jennings, D. C. Lamppa, S. B. Hansen, A. J. Harvey-Thompson, D. J. Ampleford, M. E. Cuneo, T. Strizic, D. Johnson, M. C. Jones, N. W. Moore, T. M. Flanagan, J. L. McKenney, E. M. Waisman, and C. A. Coverdale are with Sandia National Laboratories, Albuquerque, NM 87185 USA.

M. Krishnan, K. Wilson Elliott, and R. Madden are with Alameda Applied Sciences Corp., San Leandro, CA 94577 USA.

P. L. Coleman is with Evergreen Hill Sciences, Philomath, OR 97370 USA.

J. Thompson is a consultant, San Diego, CA 92106, USA.

A. Bixler is with the Univ. of California, Berkeley, Space Sciences Laboratory, Berkeley, CA 94720 USA.

J. W. Thornhill, J. L. Giuliani, Y. K. Chong, A. L. Velikovich, and A. Dasgupta are with the Naval Research Laboratory (NRL), Washington, DC 20375 USA.

J. P. Apruzese is a consultant to NRL through Engility Corp., Chantilly, VA 20151 USA.

I. Introduction

Z-PINCH IMPLOSIONS on Sandia's Z machine [1] are extremely efficient sources of K-shell x-rays in the 1-10 keV photon energy range, producing yields up to hundreds of kilojoules [2]. Magnetically-driven implosions of argon gas in particular have been studied on pulsed power facilities since the 1970's as a source of x-rays [3]–[6]. The preceding few decades have seen a steady progression of pulsed power technology, capable of imploding gas columns on $\sim$100 ns time scales. This is rapid enough to produce 1-2 keV electron temperatures and ionize Ar gas to the K shell (He- and H-like charge states), generating characteristic x-ray lines at $\sim$3 keV photon energy. Argon gas puff z-pinches fielded by Sze *et al.* at 15 MA on the Z accelerator achieved 275 kJ of Ar K-shell radiation [7]. Later Z experiments by Coverdale *et al.* achieved $>$300 kJ. Prior to the facility's refurbishment in 2007 [8], Z gas puffs all employed the same L3 Pulsed Sciences Division nozzle and utilized driver subsystems developed and operated by L3. Subsequent research on other facilities also matured the design of supersonic, multi-shell nozzles which mitigate magnetic Rayleigh-Taylor (MRT) instability growth by structuring the initial radial distribution of the gas [9]–[11].

In addition to Ar x-ray sources, deuterium gas puffs have been previously fielded on Z with DD neutron yields up to 3×10^{13} observed [12], [13]. Analytical calculations and numerical magnetohydrodynamic (MHD) modeling suggest that a significant fraction of these neutrons can be due to thermonuclear fusion [14]; kinetic simulations have also indicated a mix of thermonuclear and beam-target fusion in high-current z-pinches [15].

Here, we report recent progress in commissioning and testing a comprehensive gas puff system on the refurbished Z machine. Our aim is to establish a multi-year science program addressing optimization of gas puff radiation sources at high current and furthering our understanding of z-pinch physics. To this end, we have integrated the design and fabrication of the gas puff hardware with the standard Z supply chain. The operation of gas puff nozzles is fully integrated with the Z control and data acquisition systems, and is also supported in an offline laboratory for testing and mass profile characteriza-

978-1-4673-5168-3/13/$31.00 ©2013 IEEE

Report Documentation Page

Form Approved
OMB No. 0704-0188

1. REPORT DATE	2. REPORT TYPE	3. DATES COVERED
JUN 2013	**N/A**	**-**

4. TITLE AND SUBTITLE
A Renewed Capability for Gas Puff Science on Sandias Z Machine

5a. CONTRACT NUMBER
5b. GRANT NUMBER
5c. PROGRAM ELEMENT NUMBER

6. AUTHOR(S)

5d. PROJECT NUMBER
5e. TASK NUMBER
5f. WORK UNIT NUMBER

7. PERFORMING ORGANIZATION NAME(S) AND ADDRESS(ES)
Sandia National Laboratories

8. PERFORMING ORGANIZATION REPORT NUMBER

9. SPONSORING/MONITORING AGENCY NAME(S) AND ADDRESS(ES)

10. SPONSOR/MONITOR'S ACRONYM(S)
11. SPONSOR/MONITOR'S REPORT NUMBER(S)

12. DISTRIBUTION/AVAILABILITY STATEMENT
Approved for public release, distribution unlimited

13. SUPPLEMENTARY NOTES
See also ADM002371. 2013 IEEE Pulsed Power Conference, Digest of Technical Papers 1976-2013, and Abstracts of the 2013 IEEE International Conference on Plasma Science. IEEE International Pulsed Power Conference (19th). Held in San Francisco, CA on 16-21 June 2013., The original document contains color images.

14. ABSTRACT
A comprehensive gas puff capability is being developed on the Z pulsed power generator. We describe the methodology employed for developing a gas puff load on Z, which combines characterization and modeling of the neutral gas mass flow from a supersonic nozzle, numerical modeling of the implosion of this mass profile, and experimental evaluation of these magnetic implosions on Z. We are beginning a multi-year science program to study gas puff z-pinch physics at high current, starting with an 8-cm-diameter double-shell nozzle which delivers a column of Ar gas that is imploded by the machines fast current pulse. The initial shots have been designed using numerical simulation with two radiation-magnetohydrodynamic codes. These calculations indicate that 1 mg/cm should provide optimal coupling to the driver and 1.6:1 middle:outer shell mass ratio will best balance the need for high implosion velocity against the need to mitigate the magnetic Rayleigh-Taylor instability. The models suggest 300- 500 kJ Ar K-shell yield should be achievable on Z, and we report an initial commissioning shot at lower voltage in which 250 kJ was measured. Future experiments will pursue optimization of Ar and Kr K-shell x-ray sources, study fusion in deuterium gas puffs, and investigate the physics of gas puff implosions including energy coupling, instability growth, and radiation generation.

15. SUBJECT TERMS

16. SECURITY CLASSIFICATION OF:			17. LIMITATION OF ABSTRACT	18. NUMBER OF PAGES	19a. NAME OF RESPONSIBLE PERSON
a. REPORT	b. ABSTRACT	c. THIS PAGE			
unclassified	**unclassified**	**unclassified**	**SAR**	**8**	

tion. Over the last two years, we have developed significant in-house core personnel expertise to design, test, and field gas puffs in multiple pre-shot test locations, and at the Z facility. We are developing a full suite of design and modeling codes and nozzle characterization instrumentation, and can design advanced structured gas puff loads to meet a variety of criteria in the coming years. Upcoming modeling and experiments will address MRT stabilization, plasma structure at stagnation, pinch energy coupling, radiation physics, and optimized fusion and K-shell loads.

To begin, we focus on the development of an Ar K-shell x-ray source on Z. We outline below a methodology for developing gas puff loads that couples experimentation with numerical simulations of the z-pinch implosion. Section II describes the initial nozzle configuration that has been implemented on Z and the interferometric characterization of the mass profiles produced by the supersonic nozzle. Section III describes the numerical models used to estimate K-shell yield in order to design the initial Z experiments. Finally, Section IV discusses the experimental measurements of x-ray yield, power, and spectrum on the Z machine from an initial commissioning shot.

II. Experimental Configuration

For both wire array and gas puff loads, there is generally a trade off between the desire to produce high velocities for K-shell excitation and the need to stabilize MRT growth during the implosion. Balancing these competing effects has motivated the development of multi-shell structured gas nozzles capable of introducing mass both at large initial radius and closer to the axis to enhance stability. Hammer *et al.* have proposed mass density profiles peaked on the axis of symmetry in order to best stabilize MRT [16], and Chuvatin *et al.* have discussed an on-axis plasma heating mechanism that may be enabled by the presence of a dense central column of gas [17]. Experiments on lower-current accelerators where Ar K-shell emission is inefficient have demonstrated a significant enhancement in K-shell yield through the inclusion of a central nozzle jet [9]. Optimization of the initial mass distribution is expected to be important for all gas puff loads at high current as well. In this section, we outline the experimental tools that enable the fielding of controlled mass profiles of gaseous loads on Z.

An 8-cm-diameter nozzle with two concentric annular shells was developed for initial Z gas puff experiments; this nozzle and the gas puff system architecture are described in detail by Krishnan *et al.* [18]. Figure 1(a) shows this nozzle mounted in the standard Z convolute. The supersonic flow from the nozzle provides a column of Ar gas through which the Z current pulse flows. Eighteen current return posts support a mesh of stainless steel wire that defines the upper anode 2.5 cm from the nozzle face. The current path from the Z convolute, through the final 7-mm-wide power feed gap, and through the gas is shown schematically in yellow. The resulting $\mathbf{j}\times\mathbf{B}$ force implodes the column of argon gas and generates a 2.5-cm-tall z-pinch on the axis of symmetry. The option for a dense central jet of gas as shown in Fig. 1(a) has been demonstrated offline, and will

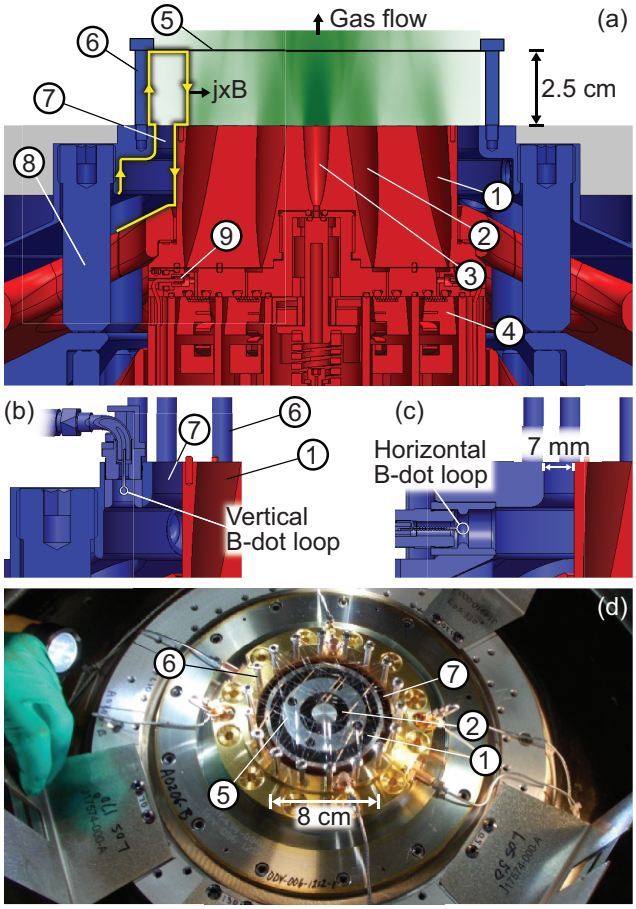

Fig. 1. (color online) (a) A section view of the Z supersonic gas nozzle, including (1) 8-cm-diameter outer annular nozzle, (2) middle annular nozzle, (3) center jet nozzle, (4) flying coil valves and gas plena, (5) anode wire grid, (6) current return posts, (7) 7-mm-wide power feed gap, (8) post-hole convolute, and (9) an in-nozzle breakdown pin. Anode components are shown in blue, and cathode components at negative potential are in red. Section views of vertical (b) and horizontal (c) B-dot current sensors are shown near the final power feed. (d) A photograph of the nozzle is shown installed in the Z machine Center Section.

be assessed in future Z shots. The initial gas puff experiment reported here fielded two annular shells, one produced from a nozzle exit aperture extending from 1-2 cm in radius, and the second from 3-4 cm.

In order to facilitate high-fidelity comparison between experiment and numerical simulation, a cathode grid was not fielded in order to avoid perturbing the gas flow in the pinch region. The effect of a cathode grid would be difficult to simulate, requiring high spatial resolution of bow shocks around each grid wire, and would introduce three-dimensional (3D) structure in the neutral gas flow that would be difficult to measure and could affect the implosion. Since a cathode grid was omitted, the nozzle was not recessed so that the surface of the nozzle would provide a well-defined cathode plane. The absence of a recess leads to relatively distinct shells of gas; assessing a more radially distributed profile will be considered

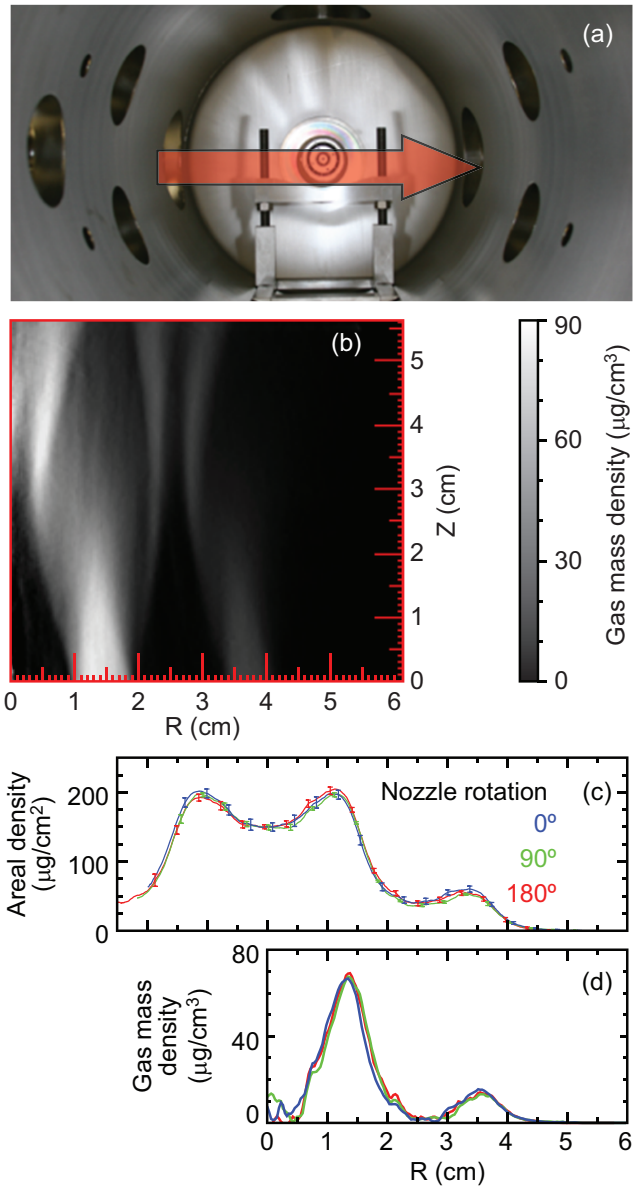

Fig. 2. (color online) (a) A 633 nm interferometer beam passes across the nozzle face inside a vacuum chamber. (b) The Abel-inverted mass density profile generated by the nozzle is measured with 400 μm spatial resolution. The nozzle face is located at Z=0, and the anode wire grid would be located at Z=2.5 cm but is absent for interferometer operation. The areal density (c) and Abel-inverted density profile (d) are shown averaged from Z=1-1.5 cm for three different azimuthal positions of the nozzle used for Z shot 2381.

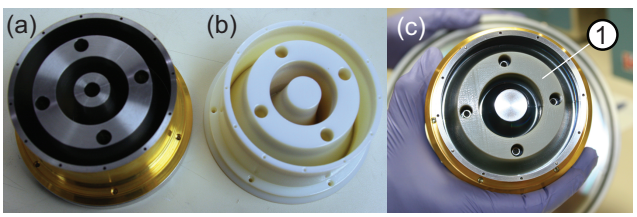

Fig. 3. (color online) The 8 cm nozzle fielded on Z fabricated in stainless steel (a) may be rapidly manufactured in plastic using 3D printing (b). When a plastic middle nozzle piece (1) was assembled with other stainless steel components (c), the measured mass profile was unchanged.

in the future. A pre-ionization system is not fielded on Z at present. Initial Z shots utilized breakdown pins mounted within the nozzle as in Fig. 1(a) to detect the presence of gas and permit Z to send energy downline. More recent gas puff shots have fielded breakdown pins 10 cm from the nozzle face above the anode grid as their operation is found to be more reliable in that configuration.

The current is measured in the magnetically insulated transmission line (MITL) section and in the feed downstream of the convolute with B-dot loop sensors [19]. The style entering the feed vertically [Fig. 1(b)] is similar to the design used on Z gas puffs prior to the refurbishment and two of these are used to infer feed current later in this report. Another style entering the feed horizontally [Fig. 1(c)] produced 10% lower peak current measurements. Accurate diagnosis of current coupled to the pinch is essential to understand energy input to the plasma and pulsed power losses, and is an area of ongoing research.

Each nozzle to be fielded on Z is characterized in advance with a Mach-Zehnder imaging interferometer designed and described by Coleman *et al.* [20]. This instrument is maintained at Sandia and will be used to test and configure nozzle hardware for Z shots as well as to develop and evaluate new nozzle designs. The fielding geometry is shown in Fig. 2(a), and an Abel-inverted mass density profile is shown in Fig. 2(b) measured with 400 μm spatial resolution. The image is obtained 950 μs after the nozzle valves are actuated, a time at which the nozzle flow is in quasi-steady state and at which Z is to be fired. We adjust the plenum pressures to select the mass and the distribution between outer and middle shells, and are able to obtain 5-10% absolute accuracy and reproducibility of the mass profile generated by the nozzles. Figure 2(c) shows areal density across the center of the pinch region for three different azimuthal positions of the nozzle. The error bars represent the standard deviation of 3-4 shots of the nozzle at each position, and the Abel-inverted profiles are compared in Fig. 2(d).

Measurements of the mass profile in this manner allow us to control the initial conditions of the gas distribution, and provide input data for numerical modeling of the implosion. Furthermore, this instrument will support the development of new nozzle designs, along with numerical modeling of the gas flow discussed in the next section. We are investigating an approach in which new nozzle contours are rapidly fabricated using 3D printing technology, tested with the interferometer, and then the design revised in order to achieve the desired gas density profile. We have used nozzle parts fabricated with a Objet 3D printer from VeroGray, a rigid opaque plastic, with 600×600×1600 dpi resolution [Fig. 3]. Fielding a middle nozzle piece of the same design as the stainless steel component but fabricated through 3D printing [Fig. 3(c)], we observed no change in mass density profiles measured by the interferometer. This suggests that rapid prototyping through 3D printing is a viable approach to iterate on nozzle design. The final nozzles to be fielded on Z would still be machined from stainless steel, as vaporizing a significant amount of plastic in the Z Center Section could harm the vacuum system.

III. Numerical Simulations

Numerical design of gas puff loads can help to define a starting point for experimental optimization, maximizing the utility of each source development shot. We have used two radiation-MHD codes to estimate the Ar K-shell yield for various configurations. Mach2-TCRE is an arbitrary Lagrangian-Eulerian, two-dimensional (2D) MHD code run for pinch physics in the r-z mode with a compressing radial grid to resolve the implosion. The simulated pinch is the inductive and resistive load of an equivalent circuit model for Z that uses Poynting's theorem for self-consistent power flow. For the non-LTE ionization kinetics of Ar it uses a tabular collisional-radiative equilibrium (TCRE) data base coupled to a probability-of-escape treatment for the opacity effects and the on-the-spot approximation for the radiation transport. This model and its application to Ar gas puffs on Z has been discussed previously by Thornhill *et al.* [21]. In addition, the 3D Eulerian MHD code Gorgon [22] is used with tabulated Ar K-shell emissivity and net opacity generated with the SCRAM atomic code [23], [24] and a single-group diffusion treatment of radiation transport.

Mach2-TCRE directly uses the mass density profiles measured interferometrically as the initial condition for the MHD simulation. The profiles are smoothed to avoid measurement noise in the data seeding unrealistically severe MRT instability early in time [21]. Thus, the degree of smoothing controls the seeding of the initial MRT perturbation. In the Gorgon modeling, a somewhat different approach is taken. The neutral gas mass flow from the nozzle is simulated hydrodynamically in Gorgon, as illustrated in Fig. 4(a) until steady-state flow is achieved, and the resulting density profile is then compared with experimental measurements as in Fig. 4(b-c). The model is calibrated against the interferometer data by adjusting the mass injection rate at the base of each nozzle. The simulated flow profile is then used as the input for the MHD implosion model, thus avoiding the impact of noise in the measured data on MRT growth but requiring the benchmarking of the hydrodynamic flow model against interferometer measurements. This hydrodynamic modeling capability, coupled with interferometric validation, will allow the design of new nozzle contours to deliver specifically tailored mass profiles in future experiments.

Random perturbations in the initial density profile are introduced to provide a seed for MRT growth in the Gorgon model. Throughout the computational volume the density is multiplied by a series of ∼400 spherically symmetric Gaussian bubbles with randomly selected amplitude, radius and position. Radii are generated between 1.5 and 4.5 mm, with amplitudes generated between 0.75 and 1.25. While the resulting MRT structures are reasonable when compared to observation, this choice of perturbation is somewhat arbitrary. Since detailed measurements of fine scale fluctuations in the gas flow are currently unavailable, work is underway to combine hydrodynamic modeling of the initial gas flow with characterization of the azimuthal variation in the throat plate at the base of the nozzle. This will allow us to determine the flow structures that may develop, and provide a more physically motivated initialization of the mass distribution. Additionally, axial and azimuthal variations in the initial radius at which breakdown first occurs are likely to have a more significant effect on seeding MRT development, so work is underway to measure and incorporate these effects.

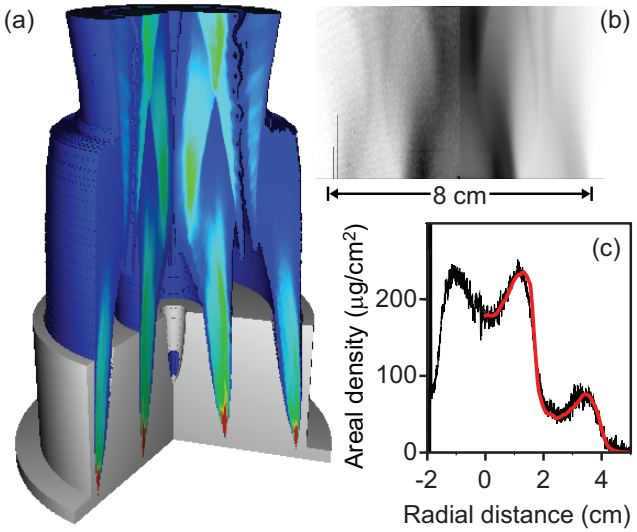

Fig. 4. (color online) (a) The mass flow from the nozzle is modeled hydrodynamically with the 3D Gorgon code until it reaches a quasi-steady state. Log density contours are shown here. (b) The simulated areal density (right half of image) is then compared to the interferometer measurement (left half) in order to validate the hydrodynamic gas flow model. (c) The measured areal density (black) is compared to the simulated areal density (red) at Z=1.2 cm from the nozzle face.

Estimated Ar K-shell yields are shown from each model in Fig. 5(a) as a function of total mass per unit length using a 1.6:1 middle:outer shell mass ratio. The Mach2-TCRE modeling preceded gas puff shots on refurbished Z, and so assumed a circuit model informed by wire array experiments using 82 kV Marx charge [21]. The circuit model in Gorgon simulations shown here use a loss model that has been informed by recent gas puff shots and uses 80 kV Marx charge. The Gorgon model predicts a peak yield at 1 mg/cm, while the Mach2-TCRE code shows yields continuing to increase with mass. This rising yield behavior has previously been seen in 1D and 2D Mach2-TCRE modeling of argon gas puffs. There is limited experimental evidence from three higher mass Ar loads at 2.4 cm length performed by Sze *et al.* [7] that show a falloff in K-shell yield at high mass loadings. Two of these shots had load mass >1.7 mg/cm for which Mach2-TCRE would predict diminished yield, and the remaining 1.2 mg/cm experiment had significant current losses. The question of whether Ar K-shell yield increases with mass loadings slightly beyond 1 mg/cm is unresolved. A future area of study will be to compare the models in order to understand why the predicted trends differ, which could be due to the influence of 3D effects at stagnation or perhaps due to differences in the radiation models employed.

In addition to total mass, we also studied the dependence of Ar K-shell yield on the ratio of masses between the shells.

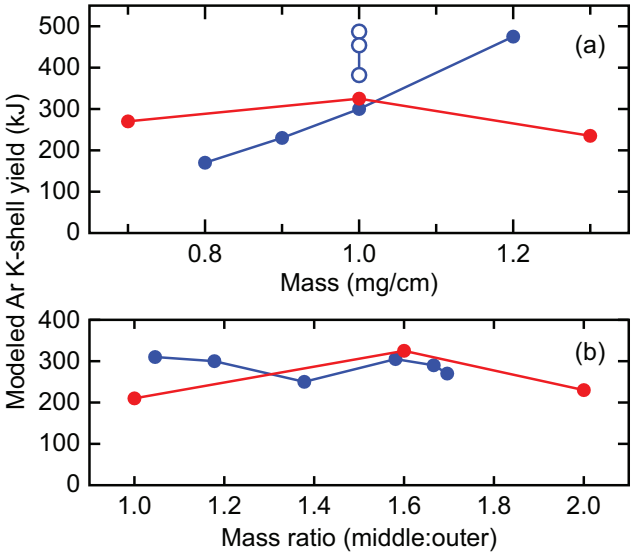

Fig. 5. (color online) Simulated Ar K-shell yield is shown versus mass (a) and versus mass ratio (b) for 3D MHD Gorgon (red) and 2D RMHD Mach2-TCRE (blue) numerical models. Mach2-TCRE simulations in (a) were also performed with a revised circuit model and higher 85 kV Marx charge using three separately measured interferometer profiles from the same nozzle (hollow blue points). All simulations in (a) had a 1.6:1 middle:outer shell mass ratio.

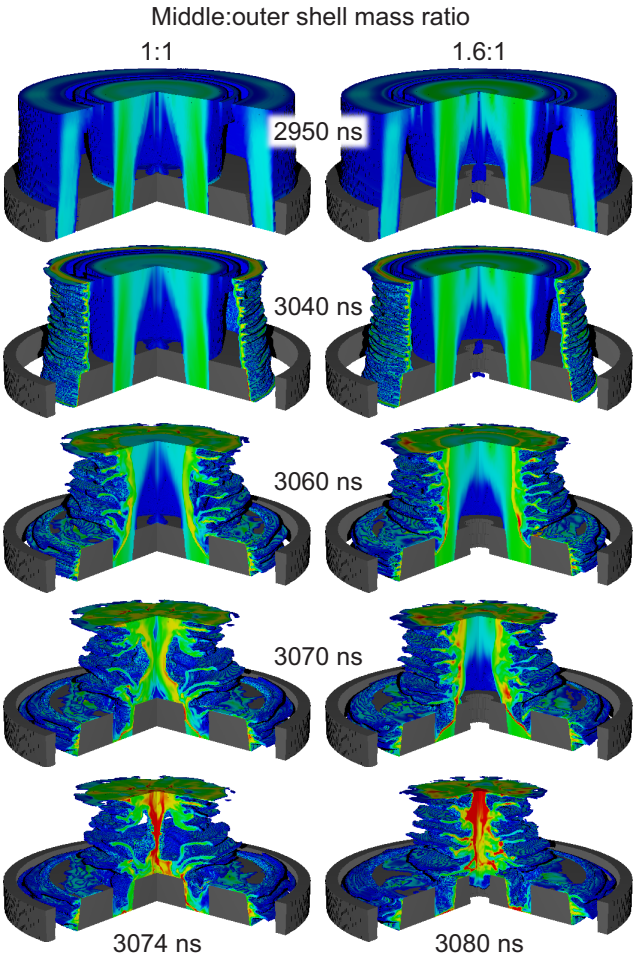

Fig. 6. (color online) Log density plots are compared for various time steps in Gorgon 3D MHD simulations of Ar gas puff implosions with 1:1 and 1.6:1 middle:outer shell mass ratios. Both models have the same initial mass in the outer shell.

While more tailored mass profiles may in fact be optimal [9]–[11], [16], [17], adjusting the shell mass ratio provides some control over MRT stabilization. Initiating all mass at large radius provides the greatest implosion velocity, however is most susceptible to MRT instability. In Fig. 5(b), the modeled yields are shown calculated versus shell mass ratio. The Mach2-TCRE simulations were scaled to 1 mg/cm total mass as the ratio between shells was adjusted, while the Gorgon calculations kept the outer shell mass fixed corresponding to 1 mg/cm at 1.6:1 ratio and then adjusted the middle shell mass in order to change the ratio in the points shown. Both codes show an optimum at 1.6:1 middle:outer shell ratio; the Mach2-TCRE models increase again toward a 1:1 ratio, but these implosions exhibit significant MRT development at stagnation which is expected to be deleterious to radiation output in the experiments (Ref. [21], Fig. 11). The role of the mass in the middle shell in stabilizing MRT evolution is illustrated for the Gorgon modeling in Fig. 6. The MRT growth accelerates dramatically as the implosion front exits the outer shell of mass, and is then stabilized when the middle shell is encountered. Greater mass in the middle shell better stabilizes the implosion, but also reduces velocity and delays the time of stagnation. The Gorgon simulations include recesses corresponding to the annular nozzle exit apertures and suggest that the implosion front may push down into the nozzle openings but that this does not adversely affect the implosion.

On the basis of the numerical simulations performed prior to the recent Z gas puff shots, we selected 1 mg/cm and 1.6:1 ratio as the initial point at which to begin experimental source development experiments at 80-85 kV Marx charge. To study sensitivity of the numerical simulation to initial conditions, we have also performed Mach2-TCRE simulations using three different interferometer measurements of this mass profile generated from the same nozzle with a higher 85 kV Marx charge and a revised circuit loss model. Other than the different interferometer data sets used to define the initial mass distribution, these simulations were identical. Shown as hollow points in Fig. 5(a), these suggest $\pm 15\%$ variability in the modeled yield. The detailed MRT bubble and spike structure that evolved during implosion was significantly different between the three cases, but evidently the final K-shell yield was only modestly sensitive. This may be due to the highly efficient nature of Ar K-shell excitation on Z, while inefficient K-shell radiators may be more sensitive to instability evolution and stagnated plasma parameters. Taken together, the numerical modeling presented above suggests that 300-500 kJ of Ar K-shell radiation should be achievable on refurbished Z using this 8 cm nozzle design. The resulting yield will be a strong function of current coupling to the z-pinch and the degree of losses observed in the convolute and final feed.

IV. Experimental Results and Discussion

Although Z presently supports routine operation at 85 kV Marx charge, we began operating the Z gas puff system at 70 kV in order to verify that debris generated during the shot did not pose a hazard to the vacuum insulator stack. Figure 7 shows measured currents and x-ray powers from the first shot at 70 kV, in which K-shell yield data from multiple photoconducting detectors [25] and resistive bolometers [26] indicated 250 kJ mean Ar K-shell yield with $\pm$15% uncertainty. The K-shell power pulse shown was measured by a PCD filtered with 2 mils aluminized Kapton normalized to the mean Ar K-shell yield, and the total x-ray power pulse is from the Total Energy and Power diagnostic [27] normalized to the yield measured with a bare gold bolometer. The mass was lowered to 0.8 mg/cm for this shot due to the significant reduction in stored energy in the Marx capacitor bank at 70 kV. We can make several observations based on this figure.

First, it highlights just how efficient an x-ray source Ar K-shell is on Z. Approximately one third of the total x-ray yield is generated by He- and H-like charge states radiating K-shell lines. At the peak of the x-ray power pulse, the z-pinch plasma is radiating over half of its power from the K shell. This is consistent with the observation of Sze *et al.* that Ar K-shell sources on Z had transitioned to an efficient radiation regime, scaling with the square of the load current [7]. In fact, at 70 kV Marx charge, the shot highlighted in Fig. 7 is comparable in mass, implosion time, coupled current, and K-shell yield to the best result of Sze *et al.*. With an increase in stored energy in the refurbished facility at Marx charges up to 85 kV, we expect to be able to increase Ar K-shell yield further. Assuming scaling with the square of the current (equivalent to assuming linear scaling with the Marx stored energy) would predict 370 kJ Ar K-shell yield at 85 kV.

Second, Fig. 7 also highlights that this gas puff configuration on Z suffers significant current loss in the convolute, with MITL and feed currents diverging about half of the way through the implosion. Whether losses in the convolute and perhaps also in the final power feed may be due to Ar gas scattering into the feed gap, gas leaking from o-ring seals at the in-nozzle breakdown pins or elsewhere, or radiation from the pinch having a line of sight into this region is a topic of current interest. If in fact the current losses scale nonlinearly with increasing Marx stored energy, this would reduce the predicted yield compared to the simple scaling mentioned above. Work is ongoing to assess Ar gas puff performance experimentally at 80-85 kV.

In Fig. 8, we show the time-integrated Ar K-shell spectrum from the same Z shot at 70 kV Marx charge, measured with a convex quartz crystal spectrometer and showing α through at least ϵ lines from He-like and H-like (Lyman series) charge states. The spectrum is normalized to be consistent with PCD and bolometer absolute yield measurements with filters ranging from 1.5 mils Be to 30 mils Kapton. Nearly 80% of the Ar K-shell yield is emitted from the He-α and Ly-α lines in the 3.0-3.4 keV range, and 30 kJ is emitted in the free-bound recombination continuum above 4.4 keV photon energy. Using the free-bound continuum as a source of higher energy

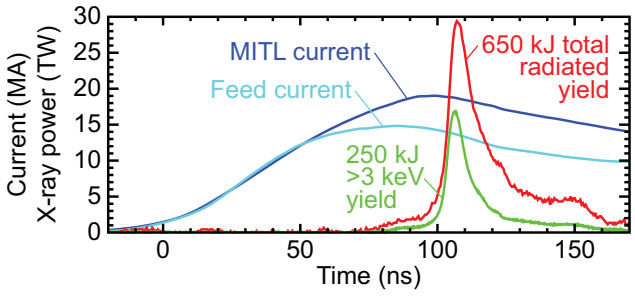

Fig. 7. (color online) Measured currents and x-ray pulses are shown from the Ar gas puff experiment performed with 70 kV Marx charge (Z2381).

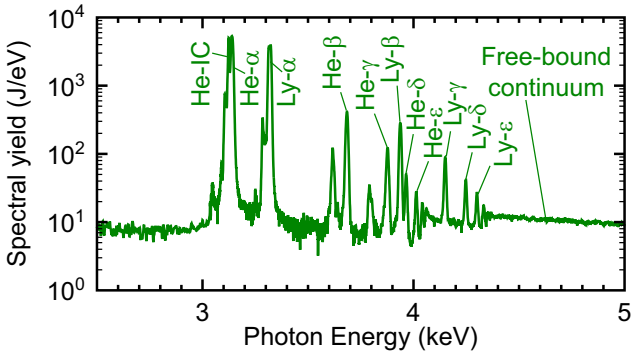

Fig. 8. (color online) The time-integrated K-shell spectrum is measured with a quartz convex crystal spectrometer using image plate as the detector, and is normalized to absolute yield measured by PCDs and bolometers (Z2381).

photons has been proposed [28], [29]; this would likely require optimization of the load for excitation of the continuum rather than K-shell line emission. Line ratio analysis of the time-integrated Ly-α and He-α + intercombination (IC) lines in the manner of Apruzese *et al.* [30] suggests $\sim$1.5 keV electron temperature, while the free-bound continuum slope suggests 2.2 keV. These temperatures are clearly more than adequate for efficient Ar K-shell excitation, and the difference in inferred temperatures is a topic of further study, perhaps related to temporal evolution of the spectrum or spatial gradients in the plasma.

Additional Z experiments will continue source development in order to optimize K-shell x-ray production and determine the shot-to-shot reproducibility of the Ar K-shell yield. In future work, we will discuss how diagnostic data including time-gated spectroscopy and imaging are being used to study the evolution of the stagnating plasma and to validate and improve the numerical simulations employed to design these initial experiments. We will continue to employ a coupled approach where both experiments and numerical simulations are used to understand stagnation dynamics, the physics of radiation generation and transport, and mitigation of MRT instability through density profile tailoring.

The methodology and instrumentation described above are part of a general capability for developing gas puff loads and studying their physics. This is being applied first to Ar K-shell sources, and will be used for Kr K-shell and deuterium fusion neutron generation with gas puff loads in the future. We

anticipate that optimizing the initial mass profile along with understanding and mitigating current losses will be important for optimizing all of these gas puff sources. Excitation of Kr K-shell emission is expected to be more difficult than for Ar, as much more coupled energy per ion is required to strip the atoms to He- and H-like charge states. The electron temperature required to ionize efficiently to the K shell is T_e (eV) $= 0.3\ Z^{2.9}$ for atomic number Z [31], thus temperatures approaching 10 keV and velocities of $\sim$150 cm/μs are desired in Kr implosions. We anticipate that these extreme conditions will drive nozzle designs toward larger diameters in order to achieve high velocities, thus making MRT stabilization more challenging. Deuterium gas puffs have additional physics associated with understanding the mechanisms of neutron production. The determination of ion temperatures is a topic which we hope to address further, along with distinguishing neutrons of thermonuclear origin from those generated by beams. Optimization of the mass density profile will also be studied for deuterium, and one interesting question is how the instability evolution differs between this less radiative, low-Z gas and the higher-Z Ar and Kr gas puffs. The gas puff capabilities being developed on Z will allow us to design experiments to continue to build understanding around these physics issues.

ACKNOWLEDGMENT

The authors would like to thank the Z machine operations and diagnostic teams for supporting these experiments, and the System Integration and Test Facility laboratory team including P. Cunningham, M. Jobe, and L. Lucero for system development, nozzle assembly, and interferometer operation. We thank Robert J. Commisso (NRL), Bruce V. Weber (NRL), Yitzhak Maron (Weizmann Institute of Science), and Amnon Fisher (Technion) for valuable advice provided during the development of the Z gas puff system. We gratefully acknowledge the Defense Threat Reduction Agency, particularly S. Seiler and J. Davis, for supporting system development including the interferometer capability, and also M. Herrmann, M. Hedemann, R. Kaye, and G. Rochau (Sandia) for their program and project support.

REFERENCES

[1] R. B. Spielman, C. Deeney, G. A. Chandler, M. R. Douglas, D. L. Fehl, M. K. Matzen, D. H. McDaniel, T. J. Nash, J. L. Porter, T. W. L. Sanford, J. F. Seamen, W. A. Stygar, K. W. Struve, S. P. Breeze, J. S. McGurn, J. A. Torres, D. M. Zagar, T. L. Gilliland, D. O. Jobe, J. L. McKenney, R. C. Mock, M. Vargas, T. Wagoner, and D. L. Peterson, *Phys. Plasmas*, vol. 5, p. 2105, 1998.

[2] C. A. Coverdale, B. Jones, D. J. Ampleford, J. Chittenden, C. Jennings, J. W. Thornhill, J. P. Apruzese, R. W. Clark, K. G. Whitney, A. Dasgupta, J. Davis, J. Giuliani, P. D. LePell, C. Deeney, D. B. Sinars, and M. E. Cuneo, *High Energy Dens. Phys.*, vol. 6, p. 143, 2010.

[3] J. Shiloh, A. Fisher, and N. Rostoker, *Phys. Rev. Lett.*, vol. 40, p. 515, 1978.

[4] C. Stallings, K. Childers, I. Roth, and R. Schneider, *Appl. Phys. Lett.*, vol. 35, p. 524, 1979.

[5] N. R. Pereira and J. Davis, *J. Appl. Phys.*, vol. 64, p. R1, 1979.

[6] R. B. Spielman and J. S. DeGroot, *Laser Part. Beams*, vol. 19, p. 509, 2001.

[7] H. Sze, P. L. Coleman, J. Banister, B. H. Failor, A. Fisher, J. S. Levine, Y. Song, E. M. Waisman, J. P. Apruzese, R. W. Clark, J. Davis, D. Mosher, J. W. Thornhill, A. L. Velikovich, B. V. Weber, C. A. Coverdale, C. Deeney, T. L. Gilliland, J. McGurn, R. B. Spielman, K. W. Struve, W. A. Stygar, and D. Bell, *Phys. Plasmas*, vol. 8, p. 3135, 2001.

[8] M. E. Savage, L. F. Bennett, D. E. Bliss, W. T. Clark, R. S. Coats, J. M. Elizondo, K. R. LeChien, H. C. Harjes, J. M. Lehr, J. E. Maenchen, D. H. McDaniel, M. F. Pasik, T. D. Pointon, A. C. Owen, D. B. Seidel, D. L. Smith, B. S. Stoltzfus, K. W. Struve, W. A. Stygar, L. K. Warne, J. R. Woodworth, C. W. Mendel, K. R. Prestwich, R. W. Shoup, D. L. Johnson, J. P. Corley, K. C. Hodge, T. C. Wagoner, and P. E. Wakeland, "An overview of pulse compression and power flow in the upgraded z pulsed power driver," in *Proc. Pulsed Power Plasma Sciences Conference*. IEEE, 2007, p. 979.

[9] H. Sze, J. Banister, B. H. Failor, J. S. Levine, N. Qi, A. L. Velikovich, J. Davis, D. Lojewski, and P. Sincerny, *Phys. Rev. Lett.*, vol. 95, p. 105001, 2005.

[10] P. L. Coleman, M. Krishnan, J. R. Thompson, J. W. Banister, B. H. Failor, J. S. Levine, N. Qi, H. M. Sze, J. P. Apruzese, J. Davis, J. W. Thornhill, A. L. Velikovich, R. J. Commisso, and A. Verma, *AIP Conf. Proc.*, vol. 808, p. 163, 2006.

[11] J. S. Levine, J. W. Banister, B. H. Failor, N. Qi, H. M. Sze, A. L. Velikovich, R. J. Commisso, J. Davis, and D. Lojewski, *Phys. Plasmas*, vol. 13, p. 082402, 2006.

[12] C. A. Coverdale, C. Deeney, A. L. Velikovich, J. Davis, R. W. Clark, Y. K. Chong, J. Chittenden, S. Chantrenne, C. L. Ruiz, G. W. Cooper, A. J. Nelson, J. Franklin, P. D. LePell, J. P. Apruzese, J. Levine, and J. Banister, *Phys. Plasmas*, vol. 14, p. 056309, 2007.

[13] C. A. Coverdale, C. Deeney, A. L. Velikovich, R. W. Clark, Y. K. Chong, J. Davis, J. Chittenden, C. L. Ruiz, G. W. Cooper, A. J. Nelson, J. Franklin, P. D. LePell, J. P. Apruzese, J. Levine, J. Banister, and N. Qi, *Phys. Plasmas*, vol. 14, p. 022706, 2007.

[14] A. L. Velikovich, R. W. Clark, J. Davis, Y. K. Chong, C. Deeney, C. A. Coverdale, C. L. Ruiz, G. W. Cooper, A. J. Nelson, J. Franklin, and L. I. Rudakov, *Phys. Plasmas*, vol. 14, p. 022701, 2007.

[15] D. R. Welch, D. V. Rose, C. Thoma, R. E. Clark, C. B. Mostrom, W. A. Stygar, and R. J. Leeper, *Phys. Plasmas*, vol. 17, p. 072702, 2010.

[16] J. H. Hammer, J. L. Eddleman, P. T. Springer, M. Tabak, A. Toor, K. L. Wong, G. B. Zimmerman, C. Deeney, R. Humphreys, T. J. Nash, T. W. L. Sanford, R. B. Spielman, and J. S. D. Groot, *Phys. Plasmas*, vol. 3, p. 2063, 1996.

[17] A. S. Chuvatin, L. I. Rudakov, A. L. Velikovich, J. Davis, and V. I. Oreshkin, *IEEE T. Plasma Sci.*, vol. 33, p. 739, 2005.

[18] M. Krishnan, K. W. Elliott, R. E. Madden, P. L. Coleman, J. R. Thompson, A. Bixler, D. C. Lamppa, J. L. McKenney, T. Strizic, D. J. adn O. Johns adn M. P. Vigil, B. Jones, D. J. Ampleford, M. E. Savage, M. E. Cuneo, and M. C. Jones, *Rev. Sci. Instrum.*, vol. 84, p. 063504, 2013.

[19] T. C. Wagoner, W. A. Stygar, H. C. Ives, T. L. Gilliland, R. B. Spielman, M. F. Johnson, P. G. Reynolds, J. K. Moore, R. L. Mourning, D. L. Fehl, K. E. Androlweicz, J. E. Bailey, R. S. Broyles, T. A. Dinwoodie, G. L. Donovan, M. E. Dudley, K. D. Hahn, A. A. Kim, J. R. Lee, R. J. Leeper, G. T. Leifeste, J. A. Melville, J. A. Mills, L. P. Mix, W. B. S. Moore, B. P. Peyton, J. L. Porter, G. A. Rochau, G. E. Rochau, M. E. Savage, J. F. Seamen, J. D. Serrano, A. W. Sharpe, R. W. Shoup, J. S. Slopek, C. S. Speas, K. W. Struve, D. M. V. D. Valde, and R. M. Woodring, *Phys. Rev. ST Accel. Beams*, vol. 11, p. 100401, 2008.

[20] P. L. Coleman, D. C. Lamppa, R. E. Madden, K. Wilson-Elliott, B. Jones, D. J. Ampleford, D. E. Bliss, C. Jennings, A. Bixler, and M. Krishnan, *Rev. Sci. Instrum.*, vol. 83, p. 083116, 2012.

[21] J. W. Thornhill, J. L. Giuliani, Y. K. Chong, A. L. Velikovich, A. Dasgupta, J. P. Apruzese, B. Jones, D. J. Ampleford, C. A. Coverdale, C. A. Jennings, E. M. Waisman, D. C. Lamppa, J. L. McKenney, M. E. Cuneo, M. Krishnan, P. L. Coleman, R. E. Madden, and K. W. Elliott, *High Energy Dens. Phys.*, vol. 8, p. 197, 2012.

[22] C. A. Jennings, M. E. Cuneo, E. M. Waisman, D. B. Sinars, D. J. Ampleford, G. R. Bennett, W. A. Stygar, and J. P. Chittenden, *Phys. Plasmas*, vol. 17, p. 092703, 2010.

[23] S. B. Hansen, J. Bauche, C. Bauche-Arnoult, and M. F. Gu, *High Energy Dens. Phys.*, vol. 3, p. 109, 2007.

[24] H. A. Scott and S. B. Hansen, *High Energy Dens. Phys.*, vol. 6, p. 39, 2010.

[25] R. B. Spielman, *Rev. Sci. Instrum.*, vol. 66, p. 867, 1995.

[26] R. B. Spielman, C. Deeney, D. L. Fehl, D. L. Hanson, N. R. Keltner, J. S. McGurn, and J. L. McKenney, *Rev. Sci. Instrum.*, vol. 70, p. 651, 1999.

[27] H. C. Ives, W. A. Stygar, D. L. Fehl, L. E. Ramirez, S. C. Dropinski, D. L. Wall, J. S. Anctil, J. S. McGurn, J. H. Pyle, D. L. Hanson, B. N. Allison, M. J. Berninger, E. A. Bryce, G. A. Chandler, M. E. Cuneo, A. J. Fox, T. L. Gilliland, C. L. Haslett, R. J. Leeper, D. F. Lewis, M. A. Lucero, M. G. Mazarakis, D. H. McDaniel, J. L. McKenney, J. A. Mills, L. P. Mix, J. L. Porter, M. B. Ritchey, L. E. Ruggles, J. F. Seamen, W. W. Simpson, R. B. Spielman, J. A. Torres, M. F. Vargas, T. C. Wagoner, L. K. Warne, and M. W. York, *Phys. Rev. ST Accel. Beams*, vol. 9, p. 110401, 2006.

[28] A. L. Velikovich, J. Davis, V. I. Oreshkin, J. P. Apruzese, R. W. Clark, J. W. Thornhill, and L. I. Rudakov, *Phys. Plasmas*, vol. 8, p. 4509, 2001.

[29] J. W. Thornhill, A. L. Velikovich, R. W. Clark, R. W. Clark, J. P. Apruzese, J. Davis, K. G. Whitney, P. L. Coleman, C. A. Coverdale, C. Deeney, B. M. Jones, and P. D. LePell, *IEEE T. Plasma Sci.*, vol. 34, p. 2377, 2006.

[30] J. P. Apruzese, K. G. Whitney, J. Davis, and P. C. Kepple, *J. Quant. Spectrosc. Radiat. Transfer*, vol. 57, p. 41, 1997.

[31] K. G. Whitney, J. W. Thornhill, J. P. Apruzese, and J. Davis, *J. Appl. Phys.*, vol. 67, p. 1725, 1990.